

# Hierarchical nanoparticle assemblies formed by decorating breath figures

ALEXANDER BÖKER<sup>1</sup>, YAO LIN<sup>1</sup>, KRISTEN CHIAPPERINI<sup>2</sup>, REINA HOROWITZ<sup>3</sup>, MIKE THOMPSON<sup>4</sup>, VINCENT CARREON<sup>5</sup>, TING XU<sup>1</sup>, CLARISSA ABETZ<sup>6</sup>, HABIB SKAFF<sup>1</sup>, A. D. DINSMORE<sup>7\*</sup>, TODD EMRICK<sup>1\*</sup> AND THOMAS P. RUSSELL<sup>1\*</sup>

<sup>1</sup>Department of Polymer Science & Engineering, University of Massachusetts, Amherst, Massachusetts 01003, USA

<sup>2</sup>Brockton High School, Brockton, Massachusetts 02301, USA

<sup>3</sup>Springfield Central High School, Springfield, Massachusetts 01109, USA

<sup>4</sup>Amherst Regional High School, Amherst, Massachusetts 01002, USA

<sup>5</sup>Physics Department, University of California, Santa Cruz, California 95064, USA

<sup>6</sup>Bayreuther Institut für Makromolekülforschung, Universität Bayreuth, 95440 Bayreuth, Germany

<sup>7</sup>Department of Physics, University of Massachusetts, Amherst, Massachusetts 01003, USA

\*e-mail: dinsmore@physics.umass.edu; tsemrick@mail.pse.umass.edu; russell@mail.pse.umass.edu

Published online: 18 April 2004; doi:10.1038/nmat1110

**T**he combination of two self-assembly processes on different length scales leads to the formation of hierarchically structured nanoparticle arrays. Here, the formation of spherical cavities, or 'breath figures'—made by the condensation of micrometre-sized water droplets on the surface of a polymer solution—that self-assemble into a well-ordered hexagonal array, is combined with the self-assembly of CdSe nanoparticles at the polymer solution–water droplet interface. Complete evaporation of the solvent and water confines the particle assembly to an array of spherical cavities and allows for *ex situ* investigation. Fluorescence confocal, transmission electron and scanning electron microscope images show the preferential segregation of the CdSe nanoparticles to the polymer solution–water interface where they form a 5–7-nm-thick layer, thus functionalizing the walls of the holes. This process opens a new route to fabricating highly functionalized ordered microarrays of nanoparticles, potentially useful in sensory, separation membrane or catalytic applications.

The phenomenon of water condensing on a clean surface to form well-ordered arrays of droplets is well known<sup>1</sup>. In the past decade, the transfer of such structures to polymer surfaces by *in situ* condensation of water droplets onto a drying polymer solution has been shown to be a convenient means to 'imprint' highly ordered honeycomb structures into polymers<sup>2,3</sup> or nanoparticle thin films<sup>4</sup>. Block copolymers and homopolymers, with and without surfactants, have been used to obtain exquisite arrays of holes, the so-called breath figures, with controlled sizes and separation distances<sup>5,6</sup>. Based on these previous investigations that established a standard method to generate breath figures with a high degree of control, in the present paper we aim to introduce functionality exclusively to the walls of the holes to enable the use of these arrays in technical applications, for example, as sensors, filters or catalytic sites. Optimizing versatility in functionalizing these surface structures requires an *ex situ* process, because *in situ* functionalization

is limited to surfactants that are compatible with the breath-figure formation. *Ex situ* processing of polymers or low-molecular-weight surfactants, however, is made difficult by the limited accessibility of the functional groups embedded in the polymer matrix, as well as the complexity of chemical reactions involved in generating new functionalities. Here, we demonstrate the use of ligand-stabilized CdSe nanoparticles to functionalize these breath-figure holes. This opens straightforward routes to modify the surface functionality within the breath figures by simple ligand exchange on the nanoparticles, thereby circumventing the above-mentioned limitations.

The self-assembly of functionalized nanoparticles yields a new route to control structural, electronic and optical properties independently by tuning the core sizes of the particles<sup>7–11</sup> and the chemistry of the attached ligands<sup>12</sup>. Earlier attempts to create periodic structures with nanoparticle decoration relied on a multi-step process involving nanoparticle-coated lattices as templates assembled into two-dimensional or three-dimensional superstructures<sup>13,14</sup>. Our approach uses the liquid–liquid interface between immiscible fluids, for example, on the surface of droplets, which has been shown to be ideal for the assembly of colloidal particles<sup>15–19</sup>. Motivated by recent experiments, where the self-assembly of ligand-stabilized nanoparticles at fluid–fluid interfaces was described<sup>19</sup>, CdSe nanoparticles were used to decorate breath figures in thin polymer films in a straightforward, one-step process, combining self-assembly on two length scales, which also allows *in situ* control over pore size and separation distance. The resulting well-ordered arrays of functionalized holes have potential use in sensor, separation or catalysis applications<sup>20,21</sup>.

To assess the standard conditions under which the breath figures were to be prepared, conditions were optimized using pure polystyrene solutions without nanoparticles. The parameters to be adjusted were the solvent, humidity in the chamber, and polymer concentration. The influence of these parameters on droplet size and separation



**Figure 1** Optical and confocal fluorescence microscope images of breath figures. **a**, Breath-figure pattern obtained with pure polystyrene. **b**, Optical and **c**, confocal fluorescence microscope images of different areas of a sample obtained from solvent-casting a polystyrene film from chloroform with CdSe nanoparticles. Scale bars: 16  $\mu\text{m}$ . The inset in **c** shows a fluorescence intensity scan along the line indicated.

distance is well-established in the literature and was used as reference<sup>2,3,5,6</sup>. Evaporation of an appropriate solvent decreases the air–liquid interfacial temperature below the dew point of water, resulting in condensation of water droplets on the polymer solution surface. After nucleation, condensation-limited growth of the droplets results in a narrow droplet-size distribution<sup>22</sup>. Subsequently, they order into a hexagonal lattice<sup>23</sup>. For our system, a humidity between 70% and 80% and a polymer concentration between 3 and 10 wt% were found to be necessary to achieve a uniform droplet size on the micrometre scale. Low humidity does not lead to water condensation. If the humidity is higher, the system disorders due to coagulation of the rapidly condensing droplets leading to a dramatic increase of the droplet size and size distribution<sup>24</sup>. The decorated breath figures presented in this work were prepared by casting a 7-wt% chloroform solution of polystyrene with 1-wt% CdSe particles (core size: 4 nm) in a humidity-controlled chamber at 80% relative humidity. Figure 1a and 1b are

optical micrographs of breath figures generated with and without the addition of nanoparticles under the same conditions. As can be seen, the size scales and characteristics of the breath figures do not depend on the presence of the nanoparticles and, therefore, the parameters that are key in the pure polymer film preparation will also be key in the case of the polymer/nanoparticle mixtures. Thus, we may assume that the droplet growth and particle segregation to the resulting liquid–liquid interface are two processes occurring simultaneously without significantly influencing each other.

Adsorption of suspended particles at the interface between immiscible liquids has been described previously for particles of micrometre<sup>18,25</sup> and nanometre<sup>19,26</sup> size. In the case of breath-figure formation from a polymer/nanoparticle solution, the condensed water droplets serve as templates for the nanoparticle assemblies. Before the polymer film becomes too viscous, the tri-*n*-octylphosphine oxide (TOPO)-stabilized CdSe nanoparticles can segregate to the interface

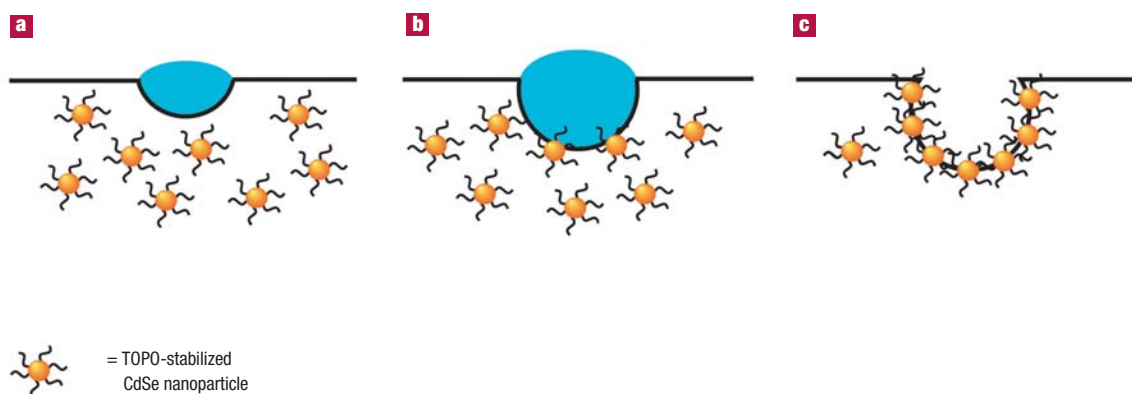


**Figure 2** Cross-sectional diagram of nanoparticle assembly at a water droplet–solution interface during the breath-figure formation. **a**, A small water droplet condenses onto the nanoparticle/polystyrene solution and **b**, sinks into the film while the particles segregate to the solution–water interface. There is no segregation to the air–solution interface. **c**, After the evaporation of the solvent and, subsequently, the water, the nanoparticles are trapped at the polymer–air interface, thereby functionalizing only the surface of the holes.

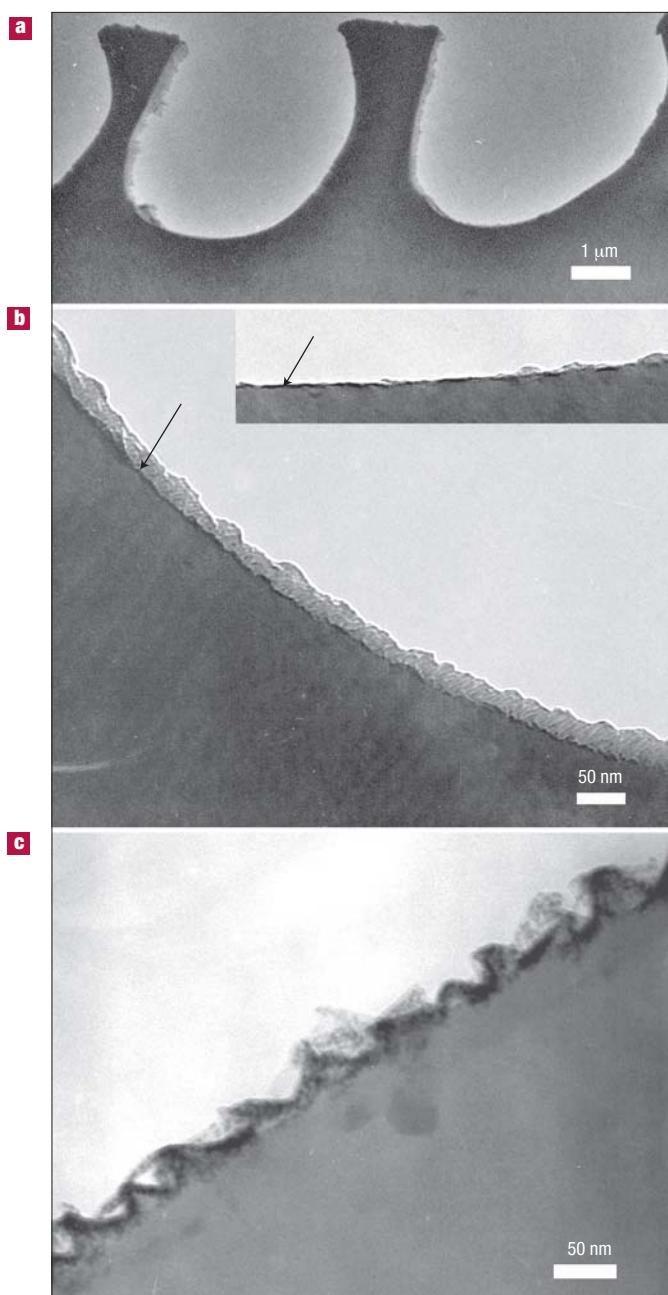


**Figure 3** TEM images of cross-sections through the porous polystyrene film. **a**, Overview of micrometre-sized holes. **b**, Magnification of the polymer–air interface, where the CdSe nanoparticles can be seen as a thin black layer (arrowed). The inset shows another spot at the polymer–air interface inside one of the holes. **c**, The CdSe nanoparticles are seen to form a ‘film’ at the polymer–air interface.

and form a uniform layer, as shown schematically in Fig. 2. As the concentration of the polymer/nanoparticle mixture increases with solvent evaporation, the film passes through the glass transition of the polymer at room temperature and locks the droplets and the nanoparticles into place. On evaporation of the water, spherical cavities remain where the walls are decorated with the nanoparticles. This permits an *ex situ* investigation of the resulting structure. Here, we note that the exact mechanism of breath-figure formation is not fully

understood and the mechanism of droplet stabilization (for example, polymer or surfactant segregation) is also under debate. Therefore, investigation of the segregation of fluorescently marked probes like the nanoparticles presented here, may open a route to elucidate the mechanisms involved. Nevertheless, such an investigation is beyond the scope of this work. Figure 1c shows a confocal fluorescence microscopic image of a dried polystyrene/nanoparticle film. The higher fluorescence intensity at the edge of the cavities shows that the particles have been trapped near the walls of the spherical cavities, that is, at the polymer–air interface within the holes. The diffuse background emission originates from nanoparticles dispersed within the polymer film.

To demonstrate further the interfacial segregation of the nanoparticles to the walls of the cavities and to elucidate their substructure, transmission electron microscopy (TEM) was performed on thin cross-sections of the polystyrene films. Figure 3a represents an overview of a part of the section. Figure 3b and 3c are taken at the polymer–air interface. In Fig. 3b, different features can be distinguished. The bright and sometimes fuzzy edge, which is also found in Fig. 3a, is attributed to a cutting artefact. The thin black line is attributed to the nanoparticle assembly produced during breath-figure formation at the liquid–liquid interface. The ~7-nm thickness of the lines corresponds essentially to a monolayer of nanoparticles, as calculated from the sum of the core diameter and associated ligands. In Fig. 3c, the polymer–air interface is magnified. The CdSe nanoparticle assembly seems to have formed a film that is disrupted and lifted by the cutting procedure during sample preparation for the TEM investigation. In addition, the observed wrinkles may be due to stress build-up during solvent evaporation and subsequent shrinkage of the polystyrene matrix. Nevertheless, single CdSe nanoparticles can be seen forming a thin layer on top of the polystyrene substrate. We assume that the lateral ordering of the nanoparticles at the surface is liquid-like, exhibiting no long-range order, as found previously in grazing-incidence small-angle X-ray scattering and TEM measurements on nanoparticle assemblies at oil–water interfaces.

Scanning electron microscope (SEM) images also yield evidence that the nanoparticles assemble only at the water–polymer interface, that is, within the holes, and not on the remaining surface of the polymer. Figure 4a and 4b show secondary electron images of the sample surface. A bright rim is seen around the opening of the cavities, originating, as in the fluorescence microscopy images, from the secondary electrons of the CdSe nanoparticles that segregated to the water–solution interface. At low magnification (Fig. 4a), it appears as if the nanoparticles are uniformly distributed throughout the sample. However, at higher magnifications (Fig. 4b, inset) it can be seen that within the spherical cavities, the walls of the cavities appear rough, or there appears to be an uneven distribution of the nanoparticles in the cavity walls. This can be attributed to the non-equilibrium nature of the solvent evaporation. It should also be noted that some of the cavities seem to have been stripped of the layer of nanoparticles during sample preparation. This suggests that the layer of assembled nanoparticles is well defined, and has mechanical properties markedly different from the polymer film, such that the entire layer coating the walls of the cavities can be removed.

To probe the CdSe nanoparticles independently, the cathodoluminescence of the sample was investigated. As seen in Fig. 4c, cathodoluminescence is predominantly found around the edges of the breath-figure holes. The rings appear fuzzy as particles not only at the rim but also deeper inside the polymer film become visible, owing to the larger penetration depth of the 7-kV primary electrons. It should also be noted that cathodoluminescence is not observed from the bottom of the spherical holes. This can be understood by considering that the signal from a monolayer of nanoparticles would be too weak to observe, and, due to a projection of the spherical shape of the cavity, there would seem to be a larger number of particles at the cavity edge.

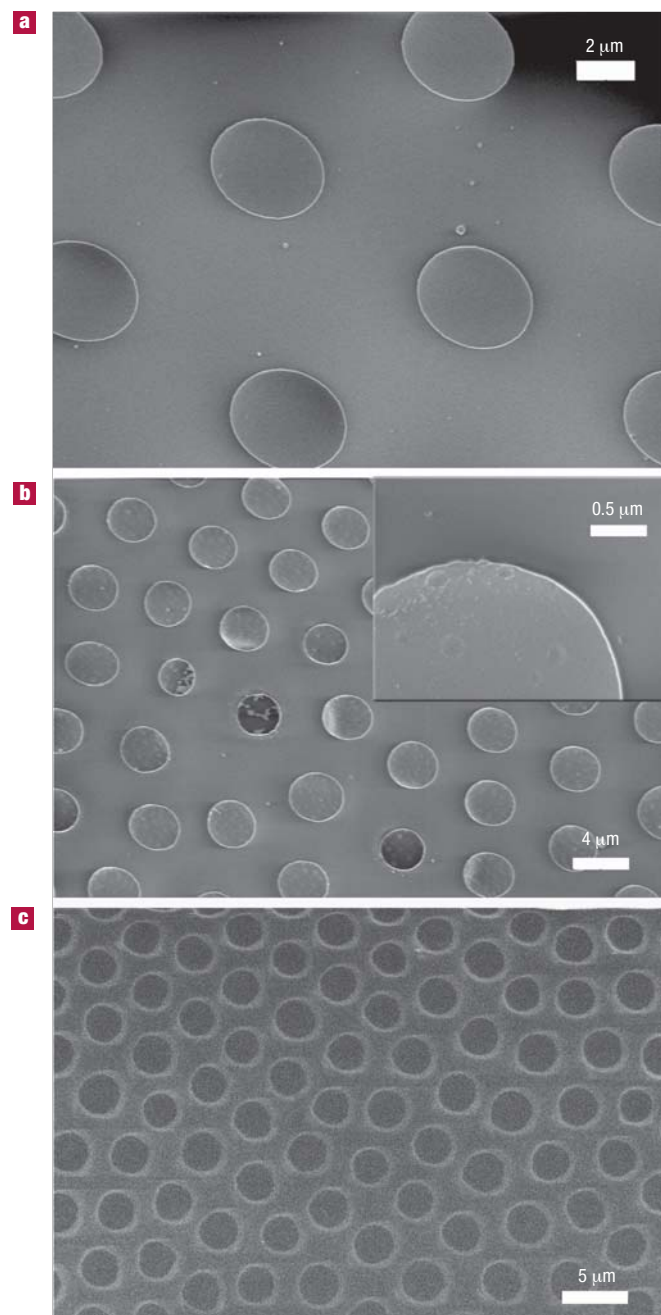


**Figure 4** Secondary-electron SEM and cathodoluminescence images of the surface of a nanoparticle-decorated breath-figure film. **a, b**, Secondary-electron SEM images of the surface of the porous polystyrene film. The bright lines show the electron emission from the CdSe. **c**, Cathodoluminescence image of the same sample. The enhanced intensity around the edges of the spherical cavities in all the images arises from the shape of the cavities and a projection of the cavity onto a planar surface, artificially enhancing the intensity at the edges.

In summary, we have described a process in which an array of spherical cavities can be imprinted into a polymer film where the walls of the cavities are decorated with CdSe nanoparticles. Modification of the ligands attached to the nanoparticles opens a simple route to functionalize the surfaces of the spherical cavities *in situ*. As the TOPO ligands are known to be replaceable with several substances including

pyridine, thiol and phosphoric acid derivatives<sup>27–29</sup>, ligands having a wide variety of functional groups, optimized for the target applications, can be considered for *ex situ* surface modification.

## METHODS

### SAMPLE PREPARATION

A 7-wt% solution of polystyrene ( $M_w = 76 \text{ kg mol}^{-1}$ , Polymer Source) in chloroform containing 1% CdSe nanoparticles (core diameter: 4.0 nm) stabilized with TOPO ligands was prepared<sup>29,30</sup>. To form the breath-figure structure, a 30- $\mu\text{l}$  drop of the solution was placed on a cover glass in a humidity-controlled chamber, and the solvents were allowed to evaporate at room temperature and 80% relative humidity. The humidity was controlled using nitrogen bubbled through a flask of distilled water at 30 °C and was measured with a digital Dickson hygrometer.

### TEM

Cross-sections of the porous films 50–80 nm thick were cut using a Leica Ultracut microtome equipped with a diamond knife. Bright-field TEM was performed on unstained samples using a JEOL 200CX electron microscope operated at 200 kV.

### LASER SCANNING CONFOCAL MICROSCOPE (LSCM)

The LSCM images were taken on a Leica TCS SP2 LSCM with an oil-immersion objective and Ar-laser excitation (excitation: 488 nm, detection: 590 nm). The optical section thickness is ~400 nm. The fluorescence from the CdSe nanoparticles is shown in a colour scale in which yellow represents the greatest intensity.

### SEM

Secondary-electron and cathodoluminescence SEM was performed using a LEO 1530 Gemini instrument equipped with a field-emission cathode. The acceleration voltage was 0.8 and 7 kV, respectively. The cathodoluminescence was detected at an angle of 30° over a wavelength range of 185–850 nm.

Received 13 January 2004; accepted 27 February 2004; published 18 April 2004.

## References

- Baker, T. J. Breath figures. *Phil. Mag.* (1798–1977) **44**, 752–765 (1922).
- Widawski, G., Rawiso, M. & Francois, B. Self-organized honeycomb morphology of star-polymer polystyrene films. *Nature* **369**, 387–389 (1994).
- Srinivasarao, M., Collings, D., Philips, A. & Patel, S. Three-dimensionally ordered array of air bubbles in a polymer film. *Science* **292**, 79–82 (2001).
- Shah, P. S. *et al.* Single-step self-organization of ordered macroporous nanocrystal thin films. *Adv. Mater.* **15**, 971–974 (2003).
- Kartha, O. *et al.* Water-assisted formation of micrometer-size honeycomb patterns of polymers. *Langmuir* **16**, 6071–6076 (2000).
- Stenzel-Rosenbaum, M. H., Davis, T. P., Fane, A. G. & Chen, V. Porous polymer films and honeycomb structures made by the self-organization of well-defined macromolecular structures created by living radical polymerization techniques. *Angew. Chem. Intl Edn* **40**, 3428–3432 (2001).
- Alivisatos, A. P. Semiconductor clusters nanocrystals and quantum dots. *Science* **271**, 933–937 (1996).
- Brus, L. Quantum crystallites and nonlinear optics. *Appl. Phys. A* **53**, 465–474 (1991).
- Lenglet, J., Bourdon, A., Bacri, J. C., Perzynski, R. & Demouchy, G. Second-harmonic generation in magnetic colloids by orientation of the nanoparticles. *Phys. Rev. B* **53**, 14941–14956 (1996).
- Alivisatos, A. P. *et al.* From molecules to materials: current trends and future directions. *Adv. Mater.* **10**, 1297–1336 (1998).
- Trindade, T., O'Brien, P. & Pickett, N. L. Nanocrystalline semiconductors: synthesis, properties, and perspectives. *Chem. Mater.* **13**, 3843–3858 (2001).
- Pileni, M. P. Nanocrystal self-assemblies: fabrication and collective properties. *J. Phys. Chem. B* **105**, 3358–3371 (2001).
- Zhang, J., Coombs, N., Kumacheva, E., Lin, Y. & Sargent, E. H. A new approach to hybrid polymer-metal and polymer-semiconductor particles. *Adv. Mater.* **14**, 1756–1759 (2002).
- Liang, Z., Susha, A. & Caruso, F. Gold nanoparticle-based core-shell and hollow spheres and ordered assemblies thereof. *Chem. Mater.* **15**, 3176–3183 (2003).
- Gaudin, A. M. *Flotation* (McGraw Hill, York, 1957).
- Pieranski, P. Two-dimensional interfacial colloidal crystals. *Phys. Rev. Lett.* **45**, 569–572 (1980).
- Velev, O. D., Furusawa, K. & Nagayama, K. Assembly of latex particles by using emulsion droplets as templates. 1. Microstructured hollow spheres. *Langmuir* **12**, 2374–2384 (1996).
- Dinsmore, A. D. *et al.* Colloidosomes: selectively permeable capsules composed of colloidal particles. *Science* **298**, 1006–1009 (2002).
- Lin, Y., Skaff, H., Emrick, T., Dinsmore, A. D. & Russell, T. P. Nanoparticles assembly and transport at liquid-liquid interfaces. *Science* **299**, 226–229 (2003).
- Nam, J.-M., Thaxton, C. S. & Mirkin, C. A. Nanoparticle-based bio-bar codes for the ultrasensitive detection of proteins. *Science* **301**, 1884–1886 (2003).
- Perez, J. M., O'Loughin, T., Simeone, F. J., Weissleder, R. & Josephson, L. DNA-based magnetic nanoparticle assembly acts as a magnetic relaxation nanoswitch allowing screening of DNA-cleaving agents. *J. Am. Chem. Soc.* **124**, 2856–2857 (2002).
- Reiss, H. The growth of uniform colloidal dispersions. *J. Chem. Phys.* **19**, 482–487 (1951).
- Gray, J. J., Harley Klein, D., Bonnecaze, R. T. & Korgel, B. A. Nonequilibrium Phase Behavior during the Random Sequential Adsorption of Tethered Hard Disks. *Phys. Rev. Lett.* **85**, 4430–4433 (2000).
- Steyer, A., Guenoun, P., Beysens, D. & Knobler, C. M. Two-dimensional ordering during droplet growth on a liquid surface. *Phys. Rev. B* **42**, 1086–1089 (1990).
- Pickering, S. Notes on the arsenates of lead and calcium. *J. Chem. Soc. Abst.* **91**, 307 (1907).
- Binks, B. P. Particles as surfactants - similarities and differences. *Curr. Opin. Colloid Interface Sci.* **7**, 21–41 (2002).

27. Lin, Y. *et al.* Ultrathin crosslinked nanoparticle membranes. *J. Am. Chem. Soc.* **125**, 12690–12691 (2003).
28. Lee, J. K., Kuno, M. & Bawendi, M. G. Surface derivatization of nanocrystalline CdSe semiconductors. *Mater. Res. Soc. Symp. Proc.* **452**, 323–328 (1997).
29. Skaff, H., Ilker, M. F., Coughlin, E. B. & Emrick, T. Preparation of cadmium selenide–polyolefin composites from functional phosphine oxides and ruthenium-based metathesis. *J. Am. Chem. Soc.* **124**, 5729–5733 (2002).
30. Murray, C. B., Kagan, C. R. & Bawendi, M. G. Synthesis and characterization of monodisperse nanocrystals and close-packed nanocrystal assemblies. *Annu. Rev. Mater. Sci.* **30**, 545–610 (2000).

#### Acknowledgements

The authors thank G. Dabkowski for assistance with the humidity chamber. This work was supported by the Department of Energy (DE-FG-02-96ER45), the National Science Foundation (NSF)-supported Materials Research Science and Engineering Center and the associated NSF-Research Experience for Teachers Program at the University of Massachusetts, Amherst (DMR 9400488), an NSF Career Award (CHE-0239486), the Eastman Kodak Company, and the MAX KADE Foundation. Correspondence and requests for materials should be addressed to T.P.R., T.E. or A.D.D.

#### Competing financial interests

The authors declare that they have no competing financial interests.